ELSEVIER

Journal of Fluids and Structures 20 (2005) 197–215

JOURNAL OF FLUIDS AND STRUCTURES

www.elsevier.com/locate/jfs

# Aeroelasticity of 2-D lifting surfaces with time-delayed feedback control

L. Librescu[a,*], P. Marzocca[b], W.A. Silva[c]

[a]*Engineering Science and Mechanics Department, Virginia Polytechnic Institute and State University, Mail cose (0219), Blacksburg, VA 24061-0219 USA*

[b]*Mechanical and Aeronautical Engineering Department, Clarkson University, Potsdam, NY 13699-5725, USA*

[c]*NASA Langley Research Center, Aeroelasticity Branch, Structures and Materials Competency, Hampton, VA 23681-2199, USA*

Received 2 February 2004; accepted 21 October 2004

**Abstract**

Two basic issues related to the open/closed-loop aeroelasticity of 2-D lifting surfaces in an incompressible flow field are considered. These concern the subcritical aeroelastic response to external time-dependent excitations, and the flutter instability of actively controlled airfoils involving a time-delayed feedback control. Results and comparisons regarding the flutter instability obtained via the first Volterra kernel in conjunction with a frequency eigenvalue analysis are presented. In the same context, the implications on the instability boundary and aeroelastic response of the presence of time-delays in the feedback control are investigated and pertinent conclusions are supplied.


## 1. Introduction

Suppression or even postponement without weight penalties of the occurrence of the flutter instability would have a great impact toward the increase of the capabilities of advanced aircraft and its ability to perform maneuvers at the edge of its operating envelope. This would result in a considerable increase of its efficiency, and at the same time, it would increase its chances of surviving in a combat environment (Marzocca et al., 2002a). These facts emphasize the importance of developing proper methodologies for the active control of flight vehicle structural systems. Their implementation would enable to increase the flutter speed, enhance the aeroelastic response by attenuating excessive vibrations, and convert the unstable limit cycle oscillation (LCO), in which case the flutter boundary is catastrophic, into a stable LCO, in which case the flutter boundary is benign. One of the limitations of the performance of the active control consists of the presence of unavoidable time-delays in controller and actuators (Palkovics et al., 1992; Ramesh and Narayanan, 2001; Hu et al., 1998). These delays can be detrimental in the sense of deteriorating the control performance, and even of precipitating the occurrence of the instability of the aeroelastic system. For a better understanding of this challenging problem, the effects of a delayed feedback control on the aeroelastic response and flutter of a 2-D airfoil is being investigated. In this context, the concept of Volterra series in conjunction with the indicial aerodynamic functions in the incompressible flight speed regime is used. The developments presented here constitute a necessary first step toward approaching the associated nonlinear aeroelastic problem.

*Corresponding author. Tel.: +1 540 231 5916; fax: +1 540 231 4574.
*E-mail address:* librescu@vt.edu (L. Librescu).

0889-9746/$ - see front matter © 2004 Elsevier Ltd. All rights reserved.
doi:10.1016/j.jfluidstructs.2004.10.005

**Nomenclature**

| | |
|---|---|
| $a$ | dimensionless elastic axis position measured from the mid-chord, positive aft |
| $b$ | semi-chord |
| $c, k$ | damping and stiffness parameters, respectively, of 1-dof plunging airfoil |
| $c_h, c_\alpha, c_\beta$ | damping parameters in plunging, pitching and flapping, respectively |
| $k_h, k_\alpha, k_\beta$ | stiffness parameters in plunging; torsional stiffnesses of the wing and flap about the elastic axis, and about the flap axis of rotation, respectively |
| $C_{L\alpha}$ | lift-curve slope, $2\pi$ |
| $C(s)$ | Theodorsen's function |
| $e$ | dimensionless leading edge flap position measured from the mid-chord, positive aft |
| $\mathbf{F_a}, \mathbf{F_b}$ | aerodynamic and time-dependent load vectors |
| $g_p, g_v$ | proportional (PFC) and velocity (VFC) feedback control gains |
| $\mathbf{G}$ | control input matrix |
| $h, \alpha, \beta$ | plunging, pitching and flap displacements, respectively |
| $I_\alpha, I_\beta$ | mass moment of inertia per unit span of the wing-flap system about the elastic axis, and of the flap about the flap axis of rotation, respectively |
| $L_a, L_b, L_c$ | aerodynamic lift, time-dependent external load, active feedback control, respectively |
| $m$ | mass of the wing per unit wing span |
| $\mathbf{M}, \mathbf{K}, \mathbf{B}$ | structural matrices, see Appendix A |
| $\mathbf{M}_a, \mathbf{K}_a, \mathbf{B}_a$ | aerodynamic matrices, see Appendix A |
| $r_\alpha, r_\beta$ | dimensionless radii of gyration of the wing-flap system, $\left(I_\alpha/mb^2\right)^{1/2}$, and of the flap, $\left(I_\beta/mb^2\right)^{1/2}$, respectively |
| $s$ | Laplace transform variable |
| $S_\alpha, \chi_\alpha$ | static unbalance about the elastic axis and its dimensionless counterpart, $S_\alpha/mb$ |
| $S_\beta, \chi_\beta$ | static unbalance about the flap axis of rotation and its dimensionless counterpart, $S_\beta/mb$ |
| $t, \sigma$ | time and dummy time variables, respectively |
| $T_i$ | Theodorsen's constants |
| $U_\infty$ | freestream speed |
| $\mathbf{x}$ | plunging, pitching and flap displacement vector |
| $\zeta_h, \zeta_\alpha, \zeta_\beta$ | structural damping ratios in plunging $\left(\equiv c_h/2m\omega_h\right)$, pitching $\left(\equiv c_\alpha/2I_\alpha\omega_\alpha\right)$, and flapping $\left(\equiv c_\beta/2I_\beta\omega_\beta\right)$, respectively |
| $\rho$ | air density |
| $\tau_i$ | time-delays, $i = 1, 2, 3, 4$ |
| $\phi(\tau)$ | Wagner's function |
| $\omega_h, \omega_\alpha, \omega_\beta$ | uncoupled frequencies in plunging, pitching and flapping, $\left(k_h/m\right)^{1/2}$, $\left(k_\alpha/I_\alpha\right)^{1/2}$, $\left(k_\beta/I_\beta\right)^{1/2}$ respectively |
| $\bar{\omega}$ | reduced frequency, $\omega b/U_\infty$ |

## 2. State of the art

The problem of controlling stable/unstable motions is an important subject in the modern mechanics, in general, and of aeroelasticity discipline, in particular. In spite of the considerable work that has been carried out in this area, many issues remain still to be clarified. One of these is related to the implication of time-delays in the feedback controls. In this context, the extensive research work concerns the study of the various aspects of dynamical systems with time-delays in the state variables and/or control inputs (Pontrjagin, 1955; Ott et al., 1990; Pyragas, 1992), and the associated stability criteria and numerical approaches [see Kolmanovskii and Nosov (1986), Stépán (1989), Marshall et al. (1992) and the references cited therein].

Moreover, time-delayed feedback control concept has been widely applied for a wheel (Palkovics and Venhovens, 1992; Ramesh and Narayanan, 2001; Hu et al., 1998; Olgac and Holm-Hansen, 1994; Hu and Wang, 1998). In Palkovics and Venhovens (1992) an investigation of the stability and chaos for wheel suspension was presented, while in Hu et al. (1998) the stability analysis has been conducted for a linear, damped single dof system, with time-delays in the displacement and the velocity feedback controls. For aeroelastic systems, with the exception of the work by Ramesh

and Narayanan (2001), the specialized literature appears to be void of any study devoted to this topic. In Ramesh and Narayanan (2001) using the feedback method of Pyragas (1992), the time-delayed feedback control of the chaotic motion of a 2-D lifting surface, with cubic pitching stiffness and linear viscous damping was carried out. From the mathematical point of view, the study of the time-delayed aeroelastic systems is more intricate than its un-delayed counterpart. In this sense, it is well known that the characteristic equation of the delayed system is transcendental. Having an infinite number of roots, it is neither possible to solve for its roots, nor to find approximate solutions easily. As a first step toward the nonlinear analysis of time-delayed aeroelastic systems, the stability of linear differential-difference aeroelastic equations has to be investigated. Such a study can provide valuable information and can answer some basic questions about the implications of the delays appearing in the feedback control on the aeroelastic response and flutter instability; and whether the system stability is robust with respect to small variations of the feedback gains and of the delays. For reasons prompted by the efficiency of the approach of nonlinear aeroelasticity via Volterra functional analysis, herein, in the linear context, the first-order kernel of Volterra series is considered. As reported in Marzocca et al. (2002a), multi-degree-of-freedom aeroelastic systems featuring structural and aerodynamic nonlinearities can be investigated via a combined Volterra series approach in conjunction with the aerodynamic indicial function technique. In Marzocca et al. (2002b) Volterra's series approach has been applied to the open/closed-loop aeroelasticity of airfoils. In that context it was shown that the method can provide an excellent basis for developing a unified and efficient approach toward addressing problems of nonlinear aeroelasticity. Within the linear approach as considered here, explicit expressions of some important quantities such as the critical time-delays and control gains, or the dependence of the transient behavior on the control parameters, are derived. Flutter instability and aeroelastic response for systems incorporating feedback control forces and moments with time-delays in the state feedback are investigated. The aeroelastic kernels including control effects are derived in terms of the structural parameters, unsteady aerodynamics, proportional (PFC) and velocity (VFC) feedback control gains and time-delays in the feedback controls. Based on these, the time histories and flutter boundary of the open/closed-loop aeroelastic system are obtained.

## 3. Analytical developments

The determination of the aeroelastic kernels, enabling one to perform open/closed-loop aeroelastic analyses that include time-delays in the control, is carried out via Volterra series approach. This methodology is theoretically well founded, simple and accurate (Rugh, 1981). Moreover, since the Volterra series approach can cope with exchange of energy between different mode frequencies (Marzocca et al., 2002a,b; Rugh, 1981), this can be considered as a promising avenue for solving various nonlinear aeroelastic problems. However, in the context of the nonlinear approach of aeroelastic systems, determination for each specific set of flight conditions of the corresponding linear and nonlinear kernels of the Volterra series is required (Marzocca et al., 2002a).

### 3.1. Single and multi degree-of-freedom aeroelastic systems

The open/closed-loop aeroelastic governing equation of an airfoil featuring plunging–pitching–flapping motion and subjected to external time-dependent loads can be expressed as

$$\mathbf{M}_s\ddot{\mathbf{x}}(t)+\mathbf{B}_s\dot{\mathbf{x}}(t)+\mathbf{K}_s\mathbf{x}(t)=\tfrac{1}{m}[\mathbf{F}_a(t)+\mathbf{F}_b(t)]+\mathbf{G}\mathbf{u}(t), \tag{1}$$

where $\mathbf{x}(t)=[h(t),\alpha(t),\beta(t)]^{\mathrm{T}}$, $\mathbf{u}(t)$ is the control input (for example, for a 3-dof, a torque applied at the flap). The unsteady aerodynamic loads are represented by

$$\mathbf{F}_a(t)=\mathbf{M}_a\ddot{\mathbf{x}}(t)+\mathbf{B}_a\dot{\mathbf{x}}(t)+\mathbf{K}_a\mathbf{x}(t)+\mathbf{F}_c(t). \tag{2}$$

The significance of the other parameters is well known; see Scanlan and Rosenbaum (1951) and Strganac et al. (2000).

The model for the system to be controlled is represented (see Özbay and Bachmann, 1994), by the transfer function $\mathrm{TF_A}$ (Fig. 1):

$$\mathrm{TF_A}=\frac{\mathbf{C_0}(s\mathbf{I}-\mathbf{A})^{-1}\mathbf{B_0}}{1-\mathbf{C_0}(s\mathbf{I}-\mathbf{A})^{-1}\mathbf{B_1}C(s)} \tag{3}$$

Herein, $\mathbf{B_0},\mathbf{B_1},\mathbf{C_0}$ are coefficients, while the transfer function of the plant of the purely linear mechanical system is represented by $\mathbf{W}=(s\mathbf{I}-\mathbf{A})^{-1}$. Moreover, when a feedback control without/with delay is included in the system, the aeroelastic system can be represented as in Figs. 2 and 3, respectively. As a remark, a closed-loop system can be seen as an open-loop system where the transfer function includes the feedback control.

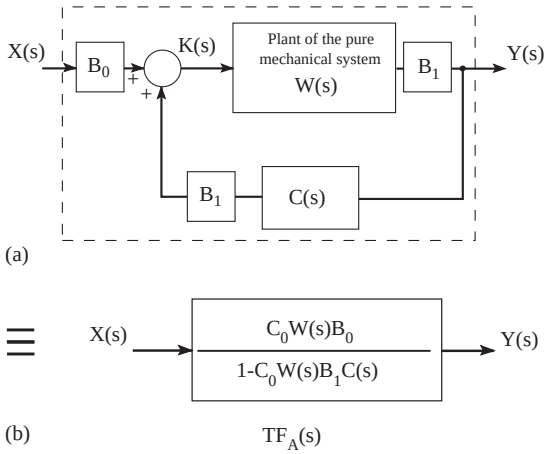


Fig. 1. Two equivalent representations of the aeroelastic system: (a) closed- and (b) open-loop systems.

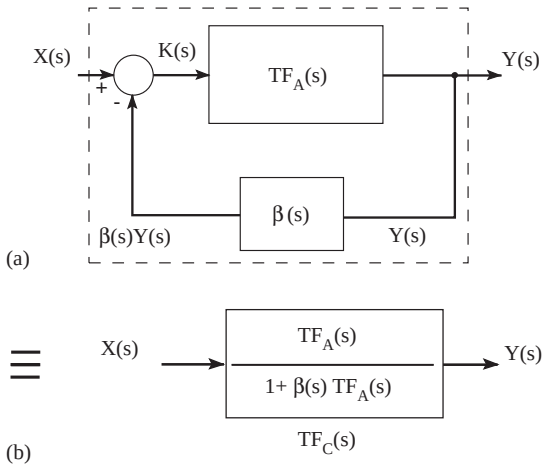


Fig. 2. Two equivalent representations of the aeroelastic system incorporating an active feedback control.

In Eq. (1) the state feedback control with delay can be expressed in the form

$$\mathbf{Gu}(t-\tau) = \mathbf{g}_p\mathbf{x}(t-\tau) + \mathbf{g}_v\dot{\mathbf{x}}(t-\tau) + \mathbf{g}_a\ddot{\mathbf{x}}(t-\tau), \tag{4}$$

where $\mathbf{g}_p, \mathbf{g}_v, \mathbf{g}_a$ are the displacement, velocity and the acceleration feedback gain matrices, respectively.

Due to the intricacy of the aeroelastic system incorporating feedback control forces and moments with time-delays in the state feedback, simplified models have been adopted in the present analysis.

### 3.2. 1-dof pure plunging airfoil

A 1-dof plunging airfoil is modeled as

$$m\ddot{h}(t) + c\dot{h}(t) + kh(t) = -L_a(t) + L_b(t) + L_c(t). \tag{5}$$

In the right-hand side member of this equation, $L_b(\tau)$ denotes the external time-dependent load acting on the rigid wing counterpart and $L_c(\tau)$ denotes the linear feedback control force

$$L_c(t) = g_p h(t) + g_v\dot{h}(t) + g_a\ddot{h}(t). \tag{6}$$

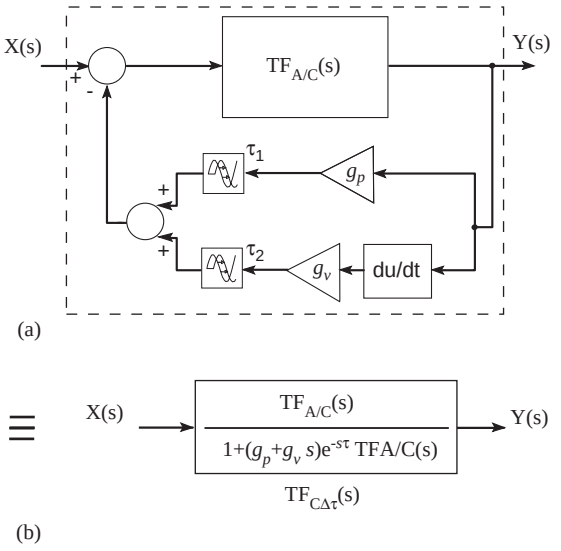


Fig. 3. Two equivalent representations of the aeroelastic system with two time-delays ($\tau_1 = \tau_2$) in the state feedback.

In the present work, only the proportional (PFC) and velocity (VFC) feedback controls have been used, implying that $g_a = 0$. In addition, for this case, the unsteady aerodynamic lift is represented by

$$L_a(t) = C_{L\alpha}\rho U_\infty b \int_0^t \phi(t-\sigma)\frac{\partial \dot{h}(\sigma)}{\partial \sigma}\,\mathrm{d}\sigma + \tfrac{1}{2}\rho C_{L\alpha} b^2 \ddot{h}. \tag{7}$$

In Eq. (7) the noncirculatory components of the unsteady aerodynamic load have been represented in terms of a convolution integral of the indicial Wagner's function $\phi(\tau)$, where the added mass is associated with the term $\frac{1}{2}\rho C_{L\alpha} b^2 \ddot{h}$. Wagner's function is connected with Theodorsen's function $C(s)$ via the Laplace transform as $C(-\mathrm{i}s) = s\int_0^\infty \phi(\tau)\mathrm{e}^{-s\tau}\,\mathrm{d}\tau$. In the R.T. Jones' approximation form, it is expressed as

$$C(s) \cong \frac{(1+0.00727059s)(1+0.0656471s)}{(1+0.0121412s)(1+0.0775765s)}, \tag{8}$$

where $C(s)\{\equiv s\Phi(s)\}$ appears in the feedback path of the aeroelastic system, meaning that the unsteady aeroelastic system can be seen as a closed-loop system fed back with the unsteady aerodynamics (see Fig. 1).

### 3.2.1. Delayed aeroelastic system: stability and response of a 1-dof airfoil

Some concepts related with the dynamic response and stability of the aeroelastic system in the presence of time-delays between the action of sensors and actuators are presented next. Considering the aeroelastic system in the absence of external loads, $L_b(\tau) = 0$, the governing equation of the system with the delayed actuator control force can be written as

$$\begin{aligned} m\ddot{h}(t) + c\dot{h}(t) + kh(t) = & -C_{L\alpha}\rho b U_\infty \int_{-\infty}^{t} \phi(t-\sigma)\ddot{h}(t)\,\mathrm{d}\sigma \\ & -\frac{1}{2}\rho C_{L\alpha} b^2 \ddot{h}(t) + g_p h(t-\tau_1) + g_v \dot{h}(t-\tau_2) \end{aligned} \tag{9}$$

Since the system is linear, the first Volterra kernel is represented as

$$H_c(s) = \left[ms^2 + cs + k + C_{L\alpha}\rho b U_\infty \Phi(s)s^2 + \frac{1}{2}\rho C_{L\alpha} b^2 s^2 + g_p \mathrm{e}^{-s\tau_1} + g_v s\mathrm{e}^{-s\tau_2}\right]^{-1}, \tag{10}$$

where the gains are taken in absolute value. Usually, in the LQG/LQR design methodologies, these gains are negative. Without aerodynamic terms (that include time-lags), and in the absence of the control (i.e. $g_p = g_v = 0$), the system is dissipative with two finite stable characteristic roots (poles) on the left half of the complex plane. However, for the aeroelastic system with feedback delayed control ($\tau_j > 0; j = 1, 2$), the two finite stable roots are supplemented by other finite stable roots (whose number depends on the aerodynamic model) and, due to the presence of $\mathrm{e}^{-s\tau}$ into the characteristic equation, by an infinite number of additional finite roots. The conditions that guarantee the stability of

the mechanical delayed system, were studied by Pontryagin (1955), and applied to stability of time-delayed feedback control systems by several authors. In the present aeroelastic analysis, Pontryagin's (1955) approach in conjunction with Stépán's (1989) theorems have been adopted.

### 3.3. 2-Dof and 3-dof airfoil

The modeling of 2 and 3-dof aeroelastic systems with time-delay feedback control can be carried out in a straightforward manner from the elements provided in Sections 3.1, 3.2 and from Section 4 where the stability of time-delay feedback aeroelastic system specialized for the 1-dof airfoil is provided.

## 4. Stépán's theorems and *D*-subdivision method: the aeroelastic stability chart

As proved in Kolmanovskii and Nosov (1986), the stability of delayed aeroelastic systems analyzed by using the concept of retarded functional differential equations (RFDE) depends on the presence of zeros with positive real part of the characteristic equation, i.e. on the presence of the *p-zeros*. For the stability evaluation, Eq. (9) can be written in a form of characteristic equation as

$$D_c(s) = 1/H_c(s) = 0. \tag{11}$$

Note that the characteristic roots, of Eq. (11) are of the form $s = a + \mathrm{i}\omega$. As a particular case, for $g_p = g_v = g$, the following relation holds:

$$g = \left\{ \left| \left[ m + C_{L\alpha}\rho b\left(U_\infty \Phi(s) + \tfrac{1}{2}b\right)\right]s^2 + cs + k \right| / |1 + s| \right\} \mathrm{e}^{a\tau}. \tag{12a}$$

From Eq. (12a) it is readily seen that for the uncontrolled system, $g_p = g_v = 0$, the characteristic equation (11) has four finite stable poles in the complex plane that are obtained by solving the equation

$$\left[ m + C_{L\alpha}\rho b\left(U_\infty \Phi(s) + \tfrac{1}{2}b\right)\right]s^2 + cs + k = 0, \tag{12b}$$

and all remaining poles are at $a = -\infty$. As a limiting case, for $g_p = g_v = \infty$ there are four finite poles that can be determined in a straightforward manner from Eq. (12a) and the remaining ones are at $a = +\infty$. For equal time-delays, via time transformation with respect to the delay, i.e. replacing $s\tau \Rightarrow \hat{s}$, Eq. (11) becomes

$$D_c(\hat{s}) = m\hat{s}^2 + c\hat{s}\tau + k\tau^2 + C_{L\alpha}\rho b U_\infty \Phi\left(\hat{s}/\tau\right)\hat{s}^2 + \tfrac{1}{2}\rho C_{L\alpha} b^2 \hat{s}^2 + g_p\tau^2 \mathrm{e}^{-\hat{s}} + g_v\tau\hat{s}\mathrm{e}^{-\hat{s}}. \tag{13}$$

The stability of Eq. (13) will be studied via Stépán's analytical method (Stépán, 1989). According to Stépán's theorem, for a system expressed as $\dot{x}(t) = \int_{-\infty}^{0}[\mathrm{d}\eta(\theta)]x(t+\theta)$, for which it is supposed that there exists a scalar $\upsilon > 0$ such that it holds the relation $\int_{-\infty}^{0} \mathrm{e}^{-\upsilon\theta}\left|\mathrm{d}\eta_{jk}(\theta)\right| < +\infty, (j,k = 1,\ldots,n)$, the characteristic function assumes the form $D_c(s) = \det(sI - \int_{-\infty}^{0} \mathrm{e}^{s\theta}\,\mathrm{d}\eta(\theta))$.

Upon denoting $\rho_1 \geq \cdots \geq \rho_r \geq 0$ and $\sigma_1 \geq \cdots \geq \sigma_s = 0$, the non-negative real zeros of

$$R(\omega) = \mathrm{Re}D_c(\mathrm{i}\omega) = (-1)^m\omega^n + \mathrm{O}(\omega^n) \tag{14a}$$

and

$$S(\omega) = \mathrm{Im}D_c(\mathrm{i}\omega) = \mathrm{O}(\omega^n), \tag{14b}$$

the trivial solution $x = 0$ of the system is exponentially asymptotically stable if and only if $R(0) > 0$; $n = 2m$ ($n$ is the order of the system and $m$ is integer); $S\left(\rho_k\right) \neq 0$ for $k = 1,\ldots,r$ and

$$\sum_{k=1}^{r} (-1)^k \mathrm{sgn}S\left(\rho_k\right) = (-1)^m m. \tag{15}$$

Similar conditions of stability are defined for systems where $n = 2m + 1$; see Hassard (1997) and Stépán (1989). It is worth noting that Hassard (1997) has provided a generalized formula for the asymptotic stability of the zero solution of delay-differential systems that counts the number of roots in the positive half-plane of the characteristic equation for general real and constant coefficient of linear delay-differential systems.

For the present case, replacing $\hat{s} \Rightarrow \mathrm{i}\omega$, $\Phi(\hat{s})\hat{s}^2 \Rightarrow C(\hat{s})\hat{s}\tau$, where $C(\bar{\omega})(\equiv F(\bar{\omega}) + \mathrm{i}G(\bar{\omega}))$ is Theodorsen's function, and considering the real and imaginary parts of Eq. (13), we obtain

$$R(\omega) = -m\omega^2 + k\tau^2 - C_{L\alpha}\rho b U_\infty G\left(\bar{\omega}/\tau\right)\omega\tau - \tfrac{1}{2}\rho C_{L\alpha} b^2\omega^2 + g_p\tau^2\cos\omega + g_v\tau\omega\sin\omega, \tag{16a}$$

$$S(\omega) = c\tau\omega + C_{L\alpha}\rho b U_\infty F\left(\bar{\omega}/\tau\right)\omega\tau - g_p\tau^2\sin\omega + g_v\tau\omega\cos\omega. \tag{16b}$$

The trivial solution of Eq. (9) is exponentially asymptotically stable, if, and only if

$$g_p > -k, \quad \tau < g_v/g_p, \tag{17a,b}$$

$$g_p < \frac{1}{\tau^2}\left\{\left[m\sigma^2 - k\tau^2 + c\sigma\tau\tan\sigma\right]\cos\sigma + C_{L\alpha}\rho b U_\infty \sigma[F\sin\sigma + G\cos\sigma]\tau + \frac{1}{2}C_{L\alpha}\rho b^2\sigma^2\cos\sigma\right\}. \tag{17c}$$

Herein, $\sigma$ is the smallest positive zero of the equation

$$S(\sigma) = c\tau\sigma + C_{L\alpha}\rho b U_\infty F\sigma\tau - g_p\tau^2\sin\sigma + g_v\tau\sigma\cos\sigma = 0, \tag{18}$$

where $\sigma \in (0, \pi/2)$. The proof of Eqs. (17) is given next.

The inequality $g_p > -k$ is obtained from the condition:

$$R(0) = k\tau^2 + g_p\tau^2 > 0. \tag{19}$$

Considering the smallest positive root $\sigma$ of Eq. (16b), such that

$$g_p\tau^2\sin\sigma = c\tau\sigma + C_{L\alpha}\rho b U_\infty F\sigma\tau + g_v\tau\sigma\cos\sigma, \tag{20}$$

one obtains that, $S(\omega) > 0, \omega \in (0, \sigma)$, if, and only if

$$c\omega + C_{L\alpha}\rho b U_\infty F\omega - g_p\tau\sin\omega + g_v\omega\cos\omega > 0, \tag{21a}$$

which yields

$$\tau < \left(c\omega + C_{L\alpha}\rho b U_\infty F\omega + g_v\omega\cos\omega\right)/\left(g_p\sin\omega\right). \tag{21b}$$

Since the first two terms of Eq. (21b) are always positive, and having in view that $\omega\cos\omega/\sin\omega < 1$ for $\omega \in (0, \pi/2)$, it is possible to conclude that the condition $\tau < g_v/g_p$ is required. In addition, for the smallest positive root $\sigma$, using the fundamental trigonometric identity, one obtains

$$R(\sigma) = -m\sigma^2 + k\tau^2 - C_{L\alpha}\rho b U_\infty G\sigma\tau - \frac{1}{2}\rho C_{L\alpha} b^2\sigma^2 + g_p\tau^2\cos\sigma + g_v\tau\sigma\sin\sigma < 0. \tag{22}$$

After straightforward algebraic manipulations, Eq. (22) in conjunction with Eq. (21b) rewritten in the form

$$g_p\tau\sin\sigma < g_v\sigma\cos\sigma + c\sigma + C_{L\alpha}\rho b U_\infty F\sigma, \tag{23}$$

reduces to Eq. (17c).

Following Stépán (1989), since $R(0) > 0$ and $\lim_{\omega\to\infty} R(\omega) \to -\infty$, $R$ has an odd number of positive zeros in $(0, \infty)$. From Eq. (22) $R$ has an odd number of positive zeros in $(0, \sigma)$ and therefore it has an even number of positive zeros in $(\sigma, \infty)$. Thus the stability condition of Eq. (15), where $m = 1$, is also fulfilled.

The approach presented here for the determination of the stability domain of a delayed aeroelastic system has some analogies with Theodorsen's method that is used for the determination of flutter speed by plotting the real and imaginary parts of the flutter determinant in conjunction with consideration of a real $\omega$. The former approach reduces to the latter one in the case of zero time-delays.

From Eq. (17c), it clearly appears that, with the increase of the stiffness parameter in plunging $k$, a decrease of the stability domain of the delayed aeroelastic system is experienced. In another context, a similar result was obtained by Palkovics and Venhovens, 1992. On the other hand, an increase of the structural damping $c$ or of the flight parameters (flight speed and density) produces an expansion of the stability domain of the delayed aeroelastic system.

## 5. Results and discussion

In this section we will analyze the stability boundary of a 1-dof airfoil, the stability and flutter boundary of a 2-dof airfoil; considerations on a 3-dof system are also provided.

### 5.1. 1-dof plunging airfoil

Some concepts related with the aeroelastic response and stability of the 1-dof plunging airfoil in the presence of time-delays between the sensing and the action of the actuator are presented next. It should be recalled, see e.g. Scanlan and Rosenbaum (1951), that due to the aerodynamic damping, such a system cannot experience flutter instability. However,

Table 1
Airfoils and flow parameters

| | |
|---|---|
| 1-dof plunging airfoil | |
| $b = 1\,ft;\ \ 0.3048\,m$ | $\rho = 0.0318\,\text{slugs/ft}^3;\ \ 16.3891\,\text{kg/m}^3$ |
| $\zeta = 0.008 \leftrightarrows$ | $c = 2m\omega\zeta \leftrightarrows$ |
| $m = 1\,\text{slugs/ft}\ \ 48.75\,\text{kg/m}$ | $k = \omega^2 m$ |
| $\omega = 60\,\text{rad/s}$ | $C_{L\alpha} = 2\pi$ |
| 2-dof plunging-pitching airfoil[a] | |
| $b = 0.135\,\text{m}$ | $\rho = 1.225\,\text{kg/m}^3$ |
| $m = 2.049\,\text{kg/m}$ | $a = -0.6847$ |
| $c_h = 27.43\,\text{kg/s} \leftrightarrows$ | $k_h = 2844.4\,\text{N/m}$ |
| $c_\alpha = 0.036\text{kg}\,\text{m}^2\text{/s}$ | $k_\alpha = 6.833\,\text{N m/rad}$ |
| $I_\alpha = mx_\alpha^2 b^2 + 0.0517\,\text{kg}\,\text{m}^2$ | $x_\alpha = \left[0.0873/b - (1+a)\right]\,\text{m}$ |
| $C_{L\alpha} = 2\pi$ | $U_F = 23.7\,\text{m/s}$ |

[a]Parameters extracted from Strganac et al. (2000).

as will be shown, due to the time-delay in the linear feedback control, an instability can be induced and the respective instability boundary can be converted via a nonlinear control from catastrophic to a benign one.

The parameters in use for the numerical simulation are presented in Table 1. The stability chart of the aeroelastic system described in Eq. (9) with respect to the feedback gains and the time-delay can be constructed using Stépán's theorem and the *D*-subdivision method. The method of *D*-subdivision is applied for determining the condition under which the quasi-polynomial $D_c(s)$, that can be expressed in the form $\sum_{l=0}^{m}\sum_{j=1}^{r} a_{lj}\mathrm{e}^{b_j s}$, where the zeros of $D_c(s)$ are continuous functions of $a_{lj}$ and $b_j$, has no *p*-zeros. The subdivision of the coefficient's $\{g_p, g_v\}$ space will be constructed by hyper surfaces, the points of which are quasi-polynomials with at least one imaginary root. It is recalled (see Kolmanovskii and Nosov, 1986), and, as proven by Kolmanovskii and Nosov (1986), that with the variation of the quasi-polynomial parameters the number of *p*-zeros may change only by passage of some zeros through an imaginary axis, and also that points of stable/unstable domains of the *D*-subdivision correspond to quasi-polynomial with the same number of *p*-zeros. The region in the $\{g_p, g_v\}$ parameter space where the roots of the characteristic equation of the system have zero real parts can be determined from the solution of

$$R(\omega) = 0 \qquad \text{and} \qquad S(\omega) = 0 \qquad \text{for} \qquad \omega \in (0, \infty), \tag{24}$$

together with the condition of Stépán's theorem. Therefore, a 3-D stability chart in the space $(g_p, g_v, \tau)$ has been represented in Fig. 4 in which the values of the geometrical parameters $\{c, k, U_\infty, m, b\}$ have been locked whereas the curves where generated via Eq. (24). The projection of this stability chart in the plane $(g_p, g_v)$ is referred in the literature to as Vyshnegradskii's diagram (Kolmanovskii and Nosov, 1986). In Table 2 a comparison of predictions with the results from Palkovics and Venhovens (1992) obtained for the vacuum conditions, is provided. The parameters used are: $k = 9000\,\text{N/m}$; $c = 0\,\text{kg/s}$; $m = 100\,\text{kg}$; $\tau = 0.03\,\text{s}$. For this simple case, a perfect agreement is reached.

Only the positive quadrant $\{g_p > 0, g_v > 0\}$ has been presented. Other stability regions can be drawn in the $\{g_p, g_v\}$ parameter space, but these are of less practical importance. As clearly appears from Fig. 4, the time-delays play an important role. It is noted that the range of stability for $g_p$ is about 330 times the one of $g_v$, implying that the stability boundary depends dramatically on the velocity feedback control, especially in the case of the time-delays. In addition, this implies that, in the presence of delay, a small variation in the velocity feedback gain can expel the system from the stable domain to the unstable domain. On the other hand, if no time-delays are present, independently of the values of the feedback gains, the stable parameter space involves the complete positive quadrant of $\{g_p, g_v\}$ parameter plane. The aeroelastic response to a step (Heaviside) load of the controlled/uncontrolled 1-dof plunging system in the presence of time-delay is represented in Figs. 5–7. The time histories presented in Figs. 5 and 6 correspond to points 1 and 2 of Fig. 4, respectively. For the assigned values of the proportional and velocity feedback gains $g_p = 5 \times 10^5\,\text{lb/ft}; 7.297 \times 10^6\,\text{N/m}$, $g_v = 1 \times 10^3\,\text{lb s/ft}; 1.460 \times 10^4\,\text{N s/m}$ and $g_p = 5 \times 10^5\,\text{lb/ft}; 7.297 \times 10^6\,\text{N/m}$, $g_v = 5 \times 10^2\,\text{lb s/ft}; 7.297 \times 10^3\,\text{N s/m}$, the system is stable (point 1), in the sense of inducing oscillations that damp out as time unfolds, and unstable (point 2), in the sense of producing an unbounded type of motion, respectively. Fig. 7 highlights the detrimental effects of the delay on the aeroelastic response. The open-loop response is presented together with the closed-loop response via the combined use of the proportional and velocity feedback control. These combined feedback

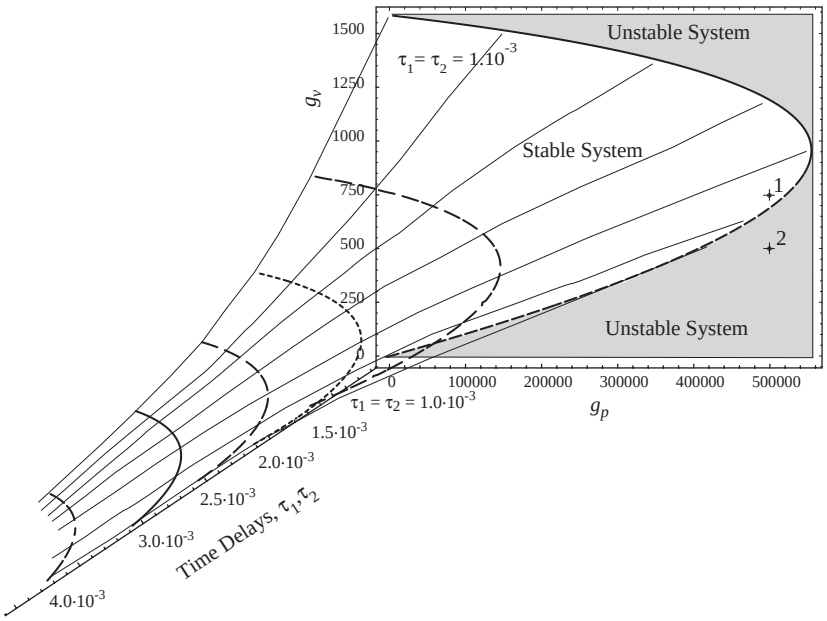


Fig. 4. Stability chart of the plunging airfoil. Effect of the time-delay.

Table 2
Stability boundary. Comparisons with Palkovics and Venhovens (1992)[a]

| $\omega$(rad/s) | $g_p$(N/m) | | $g_v$(N s/m) | |
|---|---|---|---|---|
| | Palkovics and Venhovens (1992) | Present | Palkovics and Venhovens (1992) | Present |
| $\pi/10$ | 1870.0 | 1869.99 | 58.0 | 58.02 |
| $2\pi/15$ | 9588.1 | 9588.13 | 305.7 | 305.74 |
| $\pi/6$ | 18586.4 | 18586.41 | 614.8 | 614.83 |
| $\pi/5$ | 28206.3 | 28206.30 | 978.5 | 978.47 |
| $7\pi/30$ | 37681.2 | 37681.17 | 1388.5 | 1388.53 |
| $4\pi/15$ | 46158.0 | 46158.01 | 1835.7 | 1835.74 |
| $3\pi/10$ | 52722.0 | 52722.01 | 2309.8 | 2309.84 |
| $\pi/3$ | 56423.5 | 56423.48 | 2799.7 | 2799.71 |
| $11\pi/30$ | 56306.5 | 56306.52 | 3293.6 | 3293.64 |
| $2\pi/5$ | 51438.9 | 51438.86 | 3779.4 | 3779.43 |
| $13\pi/30$ | 40942.3 | 40942.26 | 4244.7 | 4244.70 |
| $7\pi/15$ | 24022.7 | 24022.74 | 4677.0 | 4676.99 |
| $\pi/2$ | 0.0 | 0.00 | 5064.1 | 5064.10 |

[a] $g_p$ and $g_v$ correspond to $k_3$ and $k_4$ in Palkovics and Venhovens (1992).

control will be referred to as PVC. In the presence of a relatively small delay ($\tau = 0.001$ s), the oscillatory motion damps out in about 3.5 longer time than the one corresponding to the absence of delays.

The effects of natural frequency on the stability boundary of the 1-dof plunging airfoil in the presence of time-delays is presented in the 3-D stability chart, Fig. 8. Surprisingly enough, but in agreement with Eqs. (17), with an increase of the natural frequency, the domain of stability decreases; moreover, results not displayed here reveal that this effect is more prominent for larger values of the time-delay. As a limiting case, for $\tau \to 0$ the effect of the natural frequency is negligible. In addition, also from results not displayed here, it appears that for larger values of damping, larger stability domains result. As mentioned before, the present aeroelastic system does not exhibit flutter instability but exhibit a stability boundary due to the presence of the delays in the feedback control. The aerodynamic load contributes to damp

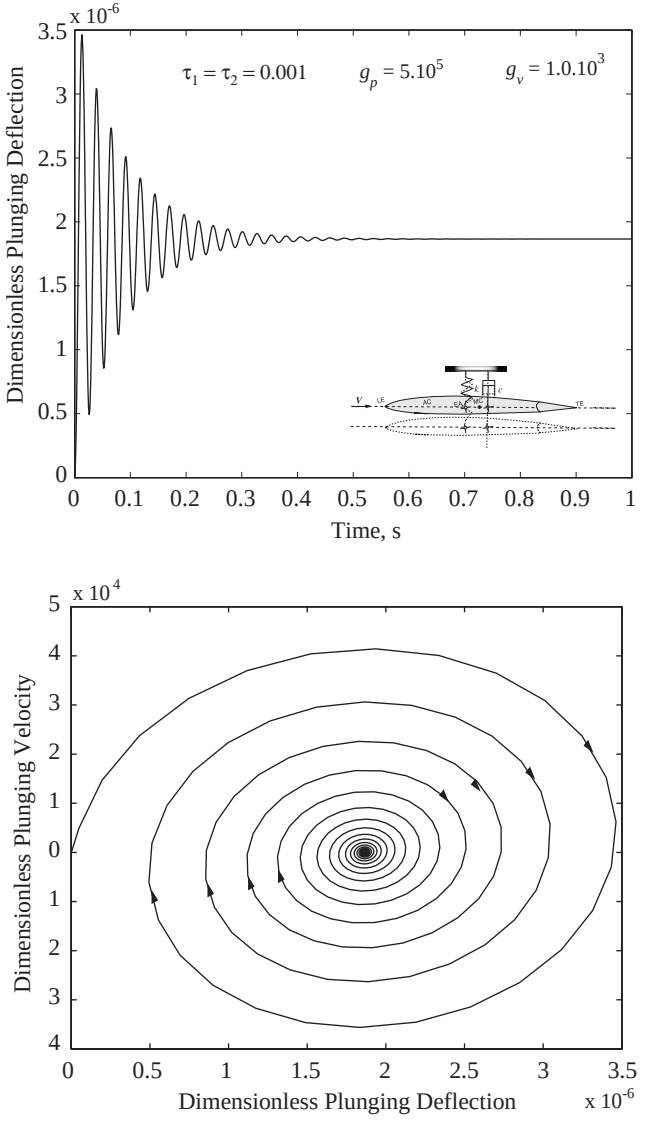


Fig. 5. Plunging time history to a step load; point 1.

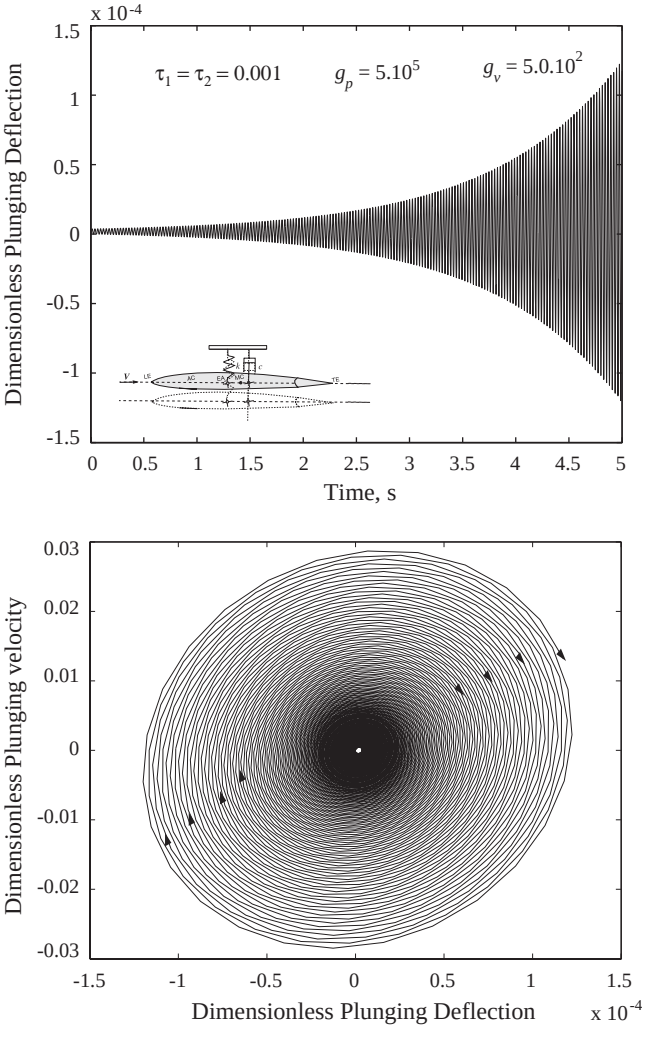


Fig. 6. Plunging time history to a step load; point 2.

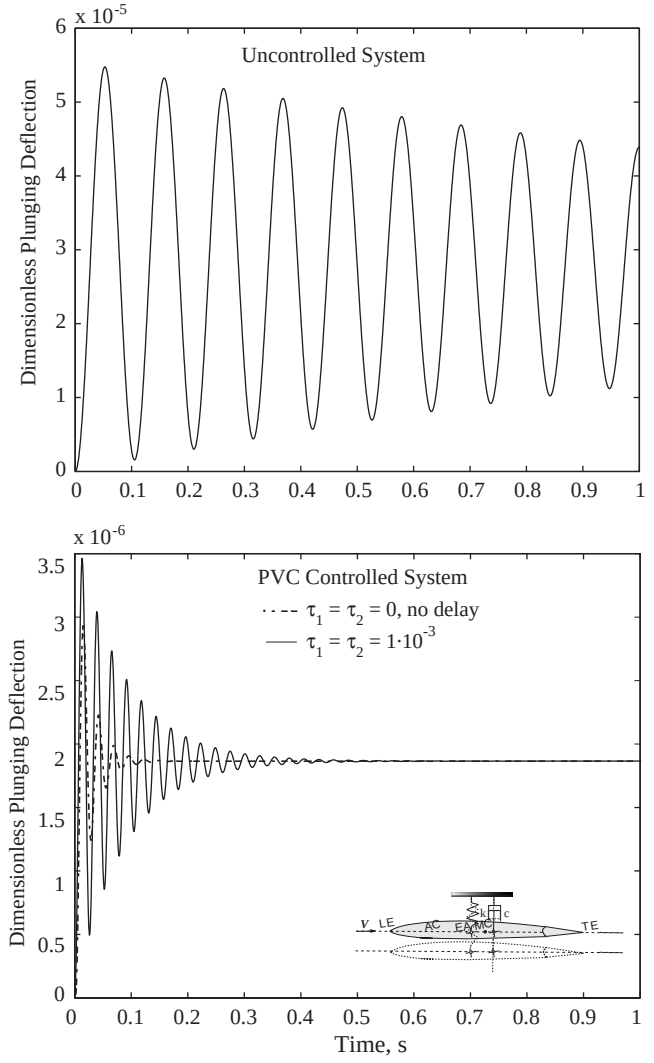


Fig. 7. Plunging time history to a step load. Open and closed-loop systems.

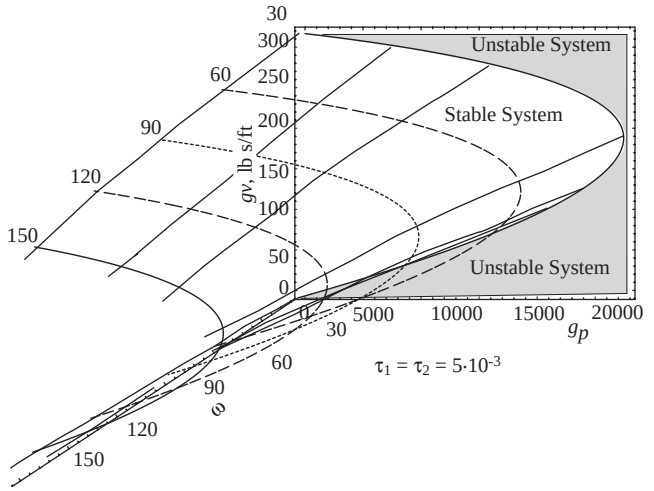


Fig. 8. Stability chart of the plunging airfoil. Effect of the natural frequency.

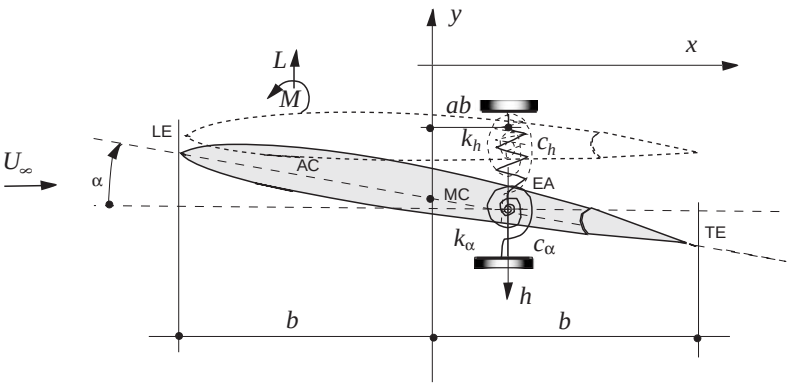


Fig. 9. Plunging–pitching airfoil.

out the airfoil motion, and so an increase in flight speed produces a slight increase in the stability domain of the aeroelastic system, and this effect is more relevant for larger values of the time-delay, implying that the stability boundary is not affected by the flight speed. However, as was shown in Fig. 4, with the decrease of the time-delay, the stable domain increases, while for zero time-delay the system does not exhibit instability at all.

### 5.2. 2-Dof plunging–pitching airfoil

A 2-dof plunging–pitching airfoil is investigated (Fig. 9). The parameters in use for the numerical simulation are presented in Table 1. In Fig. 10 the stability charts of the 2-dof airfoil in the presence of delayed proportional and velocity feedback controls in both plunging and pitching are depicted. In Fig. 10(a) two time-delays involved in the proportional and velocity feedback control related to the plunging motion have been included in the model, while in Fig. 10(b) similar delays related to the pitching motion have been incorporated. In spite of the similarity of the two graphs, the difference lies on the scale factor between the gains. The gains $g_{v\alpha}$ and $g_{p\alpha}$ are about 40 times smaller than the gains $g_{vh}$ and $g_{ph}$, respectively. This implies that the high sensitivity to the velocity feedback gain in pitching in the presence of the time-delay is a predominant factor for stability. A small variation in $g_{v\alpha}$ modifies the behavior of the system, and can even expel the stable aeroelastic system into the unstable domain. It should be pointed out that the behavior of the stability domain highly depends on the variation of the velocity feedback gain $g_{v\alpha}$. It appears that, with an increase of the gain $g_{v\alpha}$ up to the optimum value $g_{v\alpha}|_{\text{opt}} = 43.7$, the stability boundary is expanded. However, for $g_{v\alpha} > g_{v\alpha}|_{\text{opt}}$, a reduction of the stability boundary is experienced, up to another limit, larger then that corresponding to $g_{v\alpha} = 0$. In other words, Fig. 11 reveals that there exists an optimal feedback gain beyond which the stability domain sharply decreases. This issue has been pointed out in various contexts, see e.g. Librescu and Na (2001). In Figs. 12 and 13, there are presented for a 2-dof airfoil the plunging and pitching time histories for three different flight speeds, $U_\infty = 23.0, 23.7, 24.0$ m/s. The flutter speed for this airfoil is $U_F = 23.71$ m/s, implying that, for the open-loop system the motion is stable for $U_\infty < U_F$. The flutter speed $U_F$ has been determined both, via Volterra's first kernel in conjunction with the transient response and via the eigenvalue analysis. In addition, in Figs. 14–16 the plunging and pitching time histories of a 2-dof airfoil to a step load for the same three flight speeds and for selected time-delays are presented. For computational savings, for the time-delay term $e^{-\tau s}$ the stable *all-pass* approximant in the form $P(-s)/P(s)$ is used, where $P$ is a real polynomial with no zeroes in the closed right-half hand plane. In particular, the Padé-2 shift formula has been used (Niculescu, 2001):

$$e^{-\tau s} \cong \left[\left(\tau^2 s^2 - 6n\tau s + 12n^2\right)/\left(\tau^2 s^2 + 6n\tau s + 12n^2\right)\right]^n. \tag{25}$$

Other approximations, such as the Laguerre shift formula $e^{-\tau s} \cong \left[\left((\tau/2n)s - 1\right)/\left((\tau/2n)s + 1\right)\right]^n$, with $n$ sufficiently large ($>5$), can be used as well (Niculescu, 2001). The open-loop aeroelastic response is represented by a solid line, while the closed loop without delay is represented by a dotted line.

It clearly appears that, for the closed-loop system, the motion damps out even for flight speeds larger than the flutter speed. However, for small time-delays the system remains stable, but with increasing delay the response becomes unbounded, implying that an aeroelastic instability occurs.

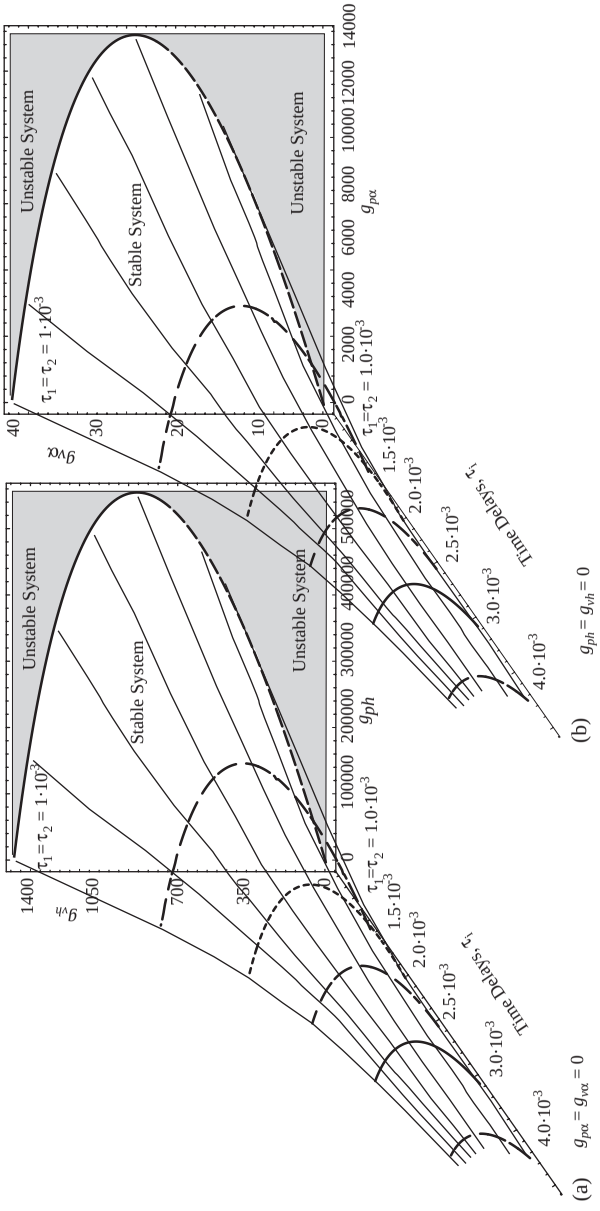


Fig. 10. Stability charts of the 2-dof plunging–pitching airfoil. Effect of the time-delay in the feedback control.

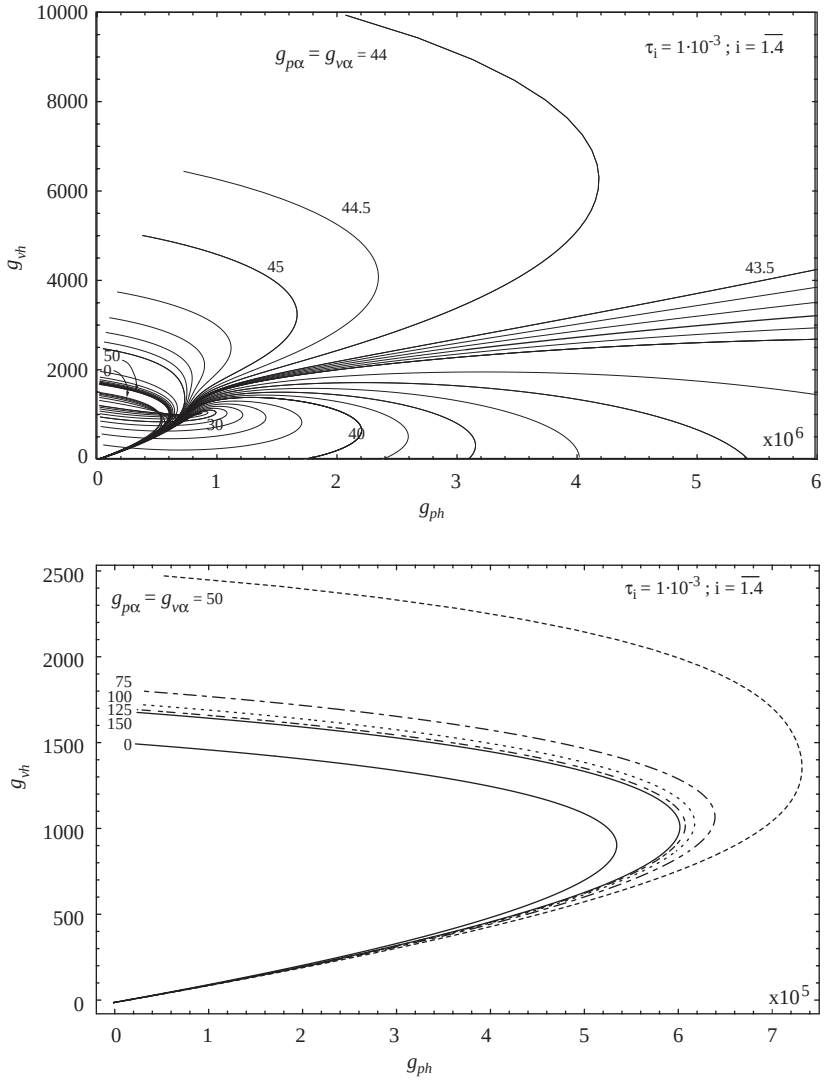


Fig. 11. Stability chart of a 2-dof airfoil.

An interesting behavior is presented in Fig. 17. The flutter speed for the uncontrolled system is 23.71 m/s, whereas for the indicated control gains, the controlled system reaches the flutter speed at 27.82 m/s. From this investigation it appears that very small time-delays are beneficial, in the sense of postponing the occurrence of the flutter instability, whereas for larger values of time-delay the system becomes unstable even for flight speeds lower than the flutter speed of the uncontrolled aeroelastic system. This trend is in full agreement with that reported in Yuan et al. (2003) where the results have been obtained via the center manifold concept. However, from the aeroelastic response point of view, the time-delay in the feedback control induces a detrimental effect, in the sense of large deflections.

### 5.3. Consideration on the 3-dof airfoil with flap

A 3-dof plunging pitching and flapping airfoil has been investigated. For the stability evaluation, the characteristic equation for the 3-dof aeroelastic system is expressed as

$$D(s) = \det \mathbf{D} = \Big|\big(\mathbf{M}_s - \tfrac{1}{m}\mathbf{M}_a\big)s^2 + \big(\mathbf{B}_s - \tfrac{1}{m}\mathbf{B}_a\big)s + \big(\mathbf{K}_s - \tfrac{1}{m}\mathbf{K}_a\big) - \tfrac{1}{m}C(\mathbf{B}_{c1} + s\mathbf{B}_{c2}) + \tfrac{1}{m}\Big(\mathbf{g}_p + s\mathbf{g}_v\Big)\mathrm{e}^{-s\tau}\Big| = 0. \tag{26}$$

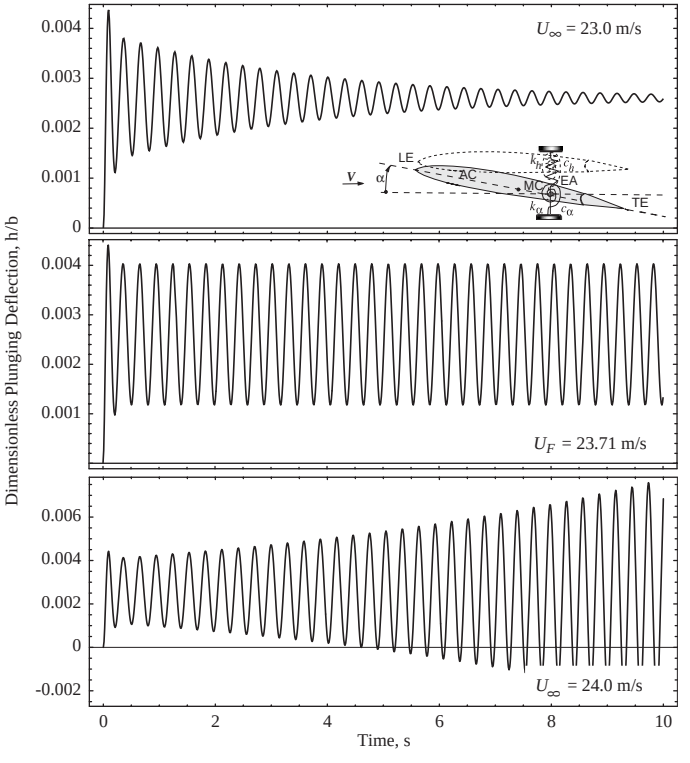


Fig. 12. Plunging time histories of the 2-dof airfoil to a step load.

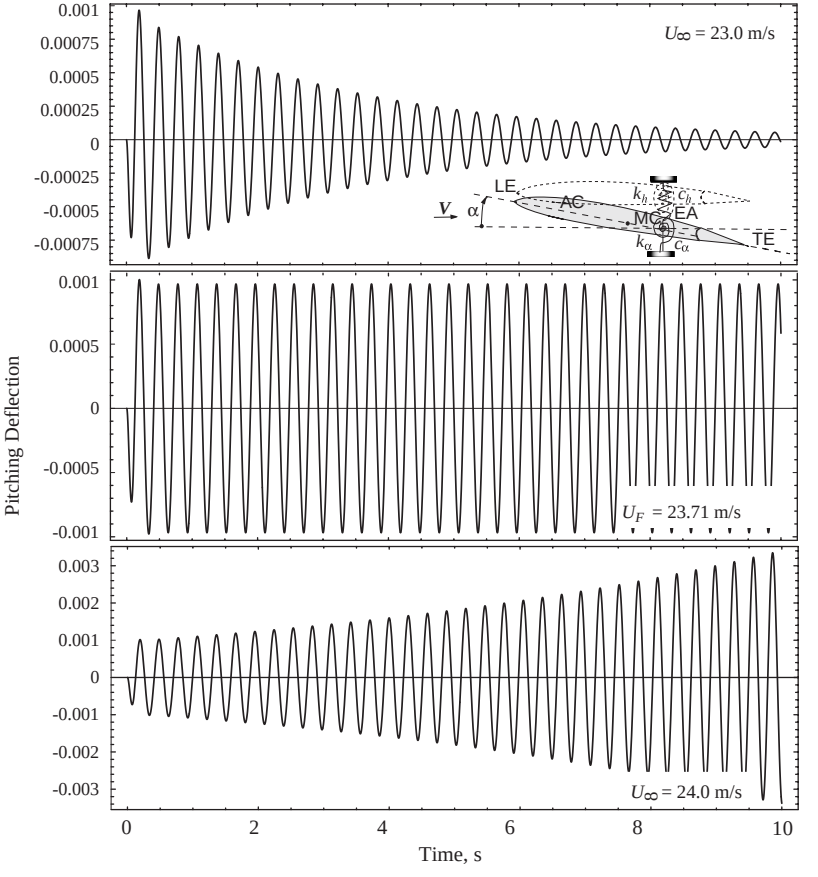


Fig. 13. Pitching time histories of the 2-dof airfoil to a step load.

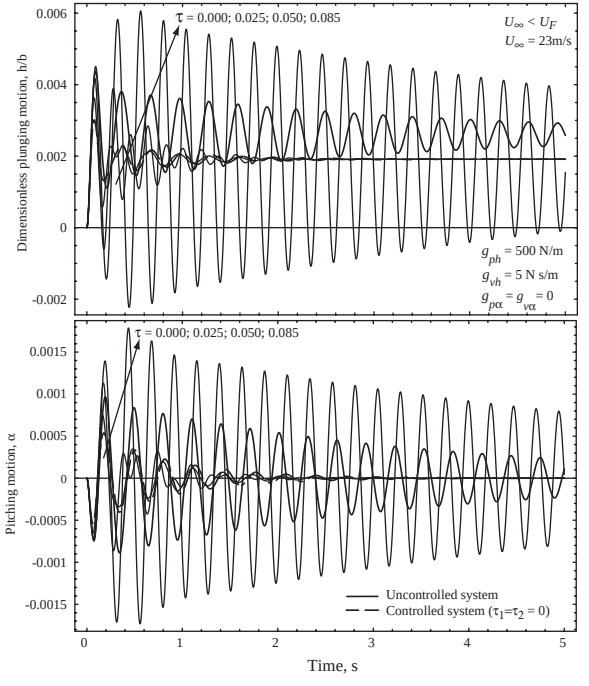


Fig. 14. Time histories of the 2-dof airfoil subjected to a step load for selected feedback time-delays $\left[U_\infty(=U_F)=23\,\mathrm{m/s}\right]$.

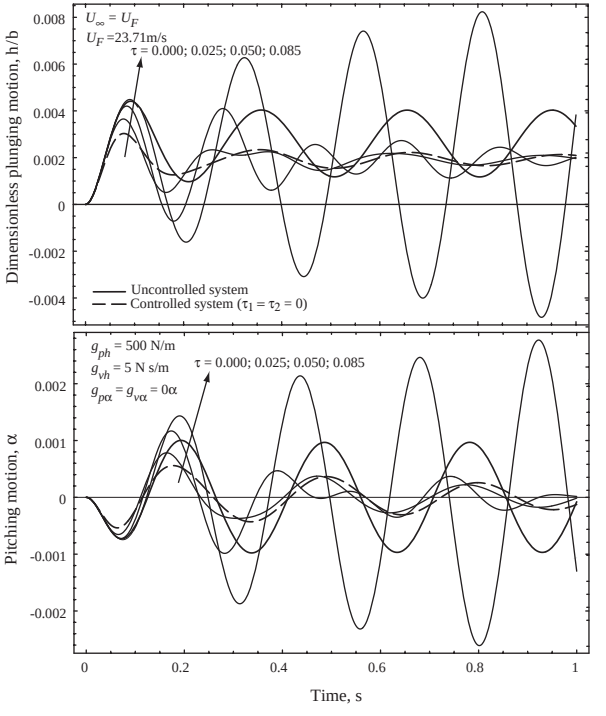


Fig. 15. Time histories of the 2-dof airfoil of the subjected to a step load for selected feedback time-delays $\left[U_\infty(=U_F)=23.71\,\mathrm{m/s}\right]$ .

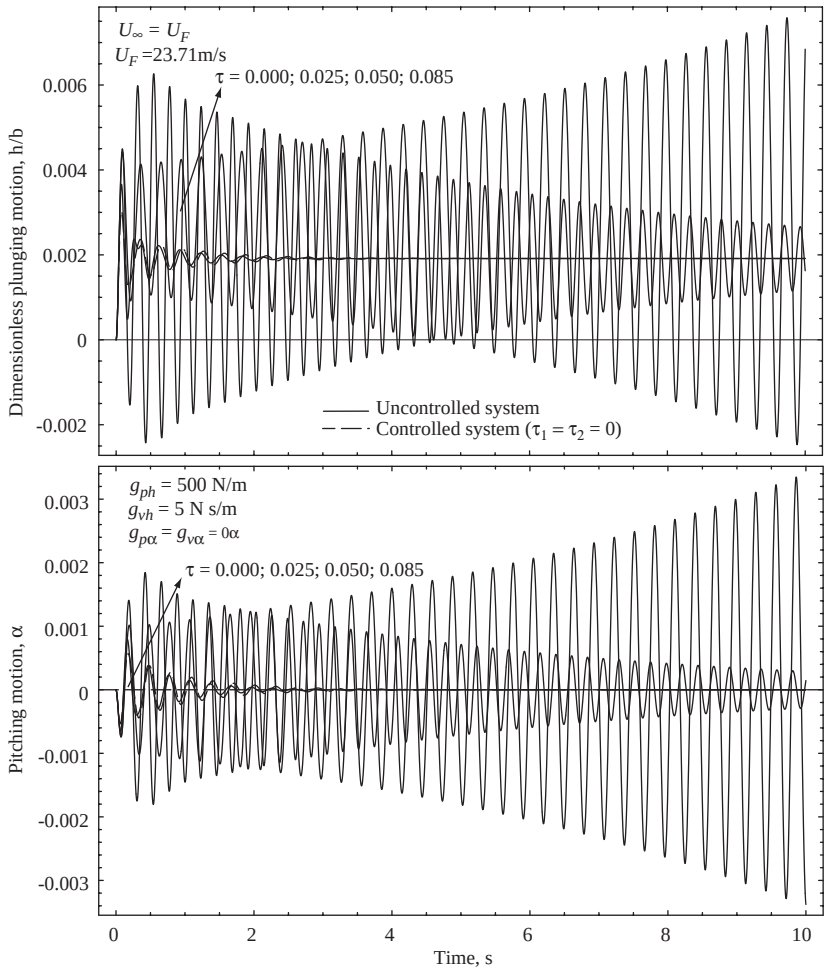


Fig. 16. Time histories of the 2-dof airfoil subjected to a step load for selected feedback time-delays $\left[U_\infty(>U_F) = 24.0\,\mathrm{m/s}\right]$.

Via the time transformation with respect to the delay, i.e. replacing $s\tau \Rightarrow \hat{s}$, Eq. (26) reduces to

$$\left|\left(\mathbf{M}_s - \tfrac{1}{m}\mathbf{M}_a\right)\hat{s}^2 + \left(\mathbf{B}_s - \tfrac{1}{m}\mathbf{B}_a\right)\hat{s}\tau + \left(\mathbf{K}_s - \tfrac{1}{m}\mathbf{K}_a\right)\tau^2 - \tfrac{1}{m}C\left(\mathbf{B}_{c1}\tau^2 + \hat{s}\tau\mathbf{B}_{c2}\right) + \tfrac{1}{m}\left(\mathbf{g}_p\tau^2 + \hat{s}\tau\mathbf{g}_v\right)\mathrm{e}^{-\hat{s}}\right| = 0. \tag{27}$$

Following the previously presented steps related to the 1-dof, and replacing $\hat{s} \Rightarrow \mathrm{i}\omega$, the real and imaginary parts of Eq. (27), can be obtained and used toward the aeroelastic stability analysis.

## 6. Conclusions

A number of results related to the aeroelasticity of a 2-D lifting surface in the presence of the time-delayed feedback control have been presented. The implications of the time-delay on the feedback control, and at the same time its complex role, have been emphasized. In this sense, it was revealed that it can be detrimental from the point of view of the aeroelastic response, for any value of the time-delay, and beneficial, from the point of view of the flutter instability, but only for small time-delays. The results reached in this paper constitute a prerequisite toward the study of nonlinear aeroelasticity for 2-D and 3-D aircraft wings and of their feedback control, featuring time-delays. With the incorporation of structural and aerodynamic nonlinearities in the aeroelastic system, more complex phenomena (involving LCOs and the chaotic motion) are likely to occur. To this end, an extension of the model presented here, based on the determination of high-order Volterra kernels, can address these issues.

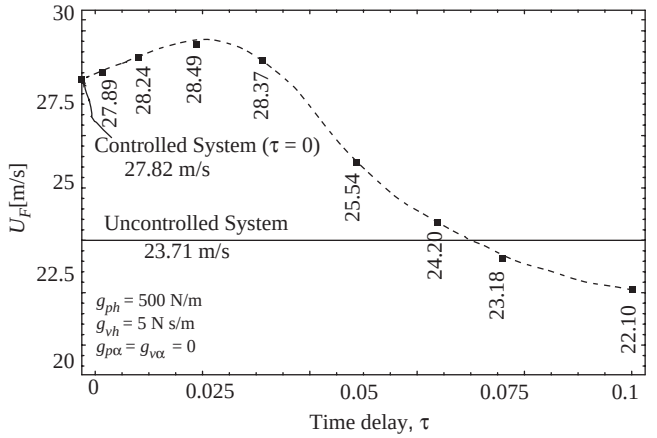


Fig. 17. Flutter boundary of the 2-dof airfoil in the presence of feedback time-delays. Controlled/ uncontrolled system.

**Acknowledgment**

The partial support of this research by the NASA Langley Research Center through Grant NAG-1-02-011 is gratefully acknowledged.

## Appendix A. Structural, aerodynamic and control matrices appearing in Eq. (1)

The matrices concerned are given by the following:

$$1-\text{DOF} \qquad 2-\text{DOF} \qquad 3-\text{DOF}$$

$$\mathbf{M} = \begin{bmatrix} 1 & bx_\alpha & bx_\beta \\ bx_\alpha & b^2 r_\alpha^2 & b^2\left[r_\beta^2 + x_\beta(e-a)\right] \\ bx_\beta & b^2\left[r_\beta^2 + x_\beta(e-a)\right] & b^2 r_\beta^2 \end{bmatrix},$$

$$\mathbf{K} = \begin{bmatrix} \omega_h^2 & 0 & 0 \\ 0 & b^2 r_\alpha^2 \omega_\alpha^2 & 0 \\ 0 & 0 & b^2 r_\beta^2 \omega_\beta^2 \end{bmatrix}, \qquad \mathbf{B} = \begin{bmatrix} 2\omega_h \zeta_h & 0 & 0 \\ 0 & 2b^2 r_\alpha^2 \zeta_\alpha \omega_\alpha & 0 \\ 0 & 0 & 2b^2 r_\beta^2 \zeta_\beta \omega_\beta \end{bmatrix},$$

$$\mathbf{M}_a = -\rho b^2 \begin{bmatrix} \pi & -\pi ba & -T_1 b \\ -\pi ba & \pi b^2\left(\frac{1}{8} + a^2\right) & -b^2[T_7 + T_1(e-a)] \\ -T_1 b & -b^2[T_7 + T_1(e-a)] & -T_3 b^2/\pi \end{bmatrix},$$

$$\mathbf{B}_a = -\rho b^2 U_\infty \begin{bmatrix} 0 & \pi & -T_4 \\ 0 & \pi b\left(\frac{1}{2} - a\right) & b\left[T_1 - T_8 - (e-a)T_4 + \frac{1}{2}T_{11}\right] \\ 0 & b\left[T_4\left(a - \frac{1}{2}\right) - T_1 - 2T_9\right] & -T_4 T_{11} b/2\pi \end{bmatrix}, \quad \mathbf{K}_a = -\rho b^2 U_\infty^2 \begin{bmatrix} 0 & 0 & 0 \\ 0 & 0 & T_4 + T_{10} \\ 0 & 0 & (T_5 - T_4 T_{10})/\pi \end{bmatrix},$$

$$\boldsymbol{A} = \begin{bmatrix} 0_{3\times 3} & \boldsymbol{I}_{3\times 3} \\ \left(\boldsymbol{M} - \frac{1}{m}\boldsymbol{M}_a\right)^{-1}\left(\frac{1}{m}\boldsymbol{K}_a - \boldsymbol{K}\right) & \left(\boldsymbol{M} - \frac{1}{m}\boldsymbol{M}_a\right)^{-1}\left(\frac{1}{m}\boldsymbol{B}_a - \boldsymbol{B}\right) \end{bmatrix},$$

$$\boldsymbol{B}_1 = \left[0_{3\times 1}\left(\boldsymbol{M} - \frac{1}{m}\boldsymbol{M}_a\right)^{-1}\boldsymbol{b}_1\right]^{\mathrm{T}}, \quad \boldsymbol{B}_0 = \left[0_{3\times 1}\left(\boldsymbol{M} - \frac{1}{m}\boldsymbol{M}_a\right)^{-1}\boldsymbol{G}\right]^{\mathrm{T}}.$$

The $T_i$ are Theodorsen's constants (Scanlan and Rosenbaum, 1951). The circulatory part of the unsteady aerodynamic load can be expressed, in the Laplace domain as

$$\hat{\mathbf{F}}_c = C(s)(\mathbf{B}_{c1} + s\mathbf{B}_{c2})\hat{\mathbf{x}}(s),$$

where

$$\mathbf{B}_{c1} = \mathbf{b_1}\mathbf{c_1}, \mathbf{B}_{c2} = \mathbf{b_1}\mathbf{c}_2, \ \mathbf{b_1} = \rho b U_\infty \begin{bmatrix} -2\pi & 2\pi b\left(a+\frac{1}{2}\right) & -T_{12}b \end{bmatrix}^{\mathrm{T}},$$

$$\mathbf{c_1} = U_\infty \begin{bmatrix} 0 & 1 & T_{10}/\pi \end{bmatrix}, \ \mathbf{c_2} = \begin{bmatrix} 1 & b\left(\frac{1}{2}-a\right) & bT_{11}/2\pi \end{bmatrix}, \ \mathbf{C}_0 = \begin{bmatrix} \mathbf{c_1} & \mathbf{c_2} \end{bmatrix}.$$

## References


Hassard, B.D., 1997. Counting roots of the characteristic equation for linear delay-differential systems. Journal of Differential Equations 136, 222–235.

Hu, H.Y., Dowell, E.H., Virgin, L.N., 1998. Stability estimation of high dimensional vibrating systems under state delay feedback control. Journal of Sound and Vibration 214, 497–511.

Hu, H.Y., Wang, Z.H., 1998. Stability analysis of damped sdof systems with two time-delays in state feedback. Journal of Sound and Vibration 214, 213–225.

Kolmanovskii, V. B., Nosov, V. R., 1986. Stability of Functional Differential Equations, vol. 180, Mathematics in Science and Engineering. Academic Press, London, UK.

Librescu, L., Na, S., 2001. Active vibration control of doubly tapered thin-walled beams using piezoelectric actuation. Thin-Walled Structures 39, 65–82.

Marshall, J. E., Górecki, Walton, K., Korytowski, A., 1992. In: Bell G.M. (Editor.), Time-Delay Systems, Stability and Performance Criteria with Applications, Series in Mathematics and its Applications. Ellis Horwood Ltd, Chichester, West Sussex, England.

Marzocca, P., Librescu, L., Silva, W.A., 2002a. Aeroelastic response of nonlinear wing section by functional series technique. AIAA Journal 40, 811–824.

Marzocca, P., Librescu, L., Silva, W. A., 2002b. Open/closed-loop nonlinear aeroelasticity for airfoils via Volterra series approach. AIAA Paper 2002-1484, 43rd AIAA/ASME/ASCE/ AHS/ASC Structures, Structural Dynamics, and Materials Conference, April 22–25, Denver, CO, USA.

Niculescu, S.-J., 2001. Delay Effects on Stability, A Robust Control Approach, Lecture Notes in Control and Information Sciences, vol. 269. Springer, London.

Olgac, N., Holm-Hansen, B.T., 1994. A novel active vibration absorption technique: delayed resonator. Journal of Sound and Vibration 176, 93–104.

Ott, E., Grebogi, C., Yorke, J.A., 1990. Controlling chaos. Physical Review Letters 64, 1196–1199.

Özbay, H., Bachmann, G.R., 1994. $H^2/H^\infty$ controller design for a two-dimensional thin airfoil flutter suppression. Journal of Guidance, Control, and Dynamics 17, 722–728.

Palkovics, L., Venhovens, P.J.Th., 1992. Investigation on stability and possible chaotic motions in the controlled wheel suspensions systems. Vehicle System Dynamics 21, 269–296.

Pontrjagin, L.S., 1955. On the zeros of some elementary transcendental functions. American Mathematical Society Translations 2, 95–110.

Pyragas, K., 1992. Continuous control of chaos by self-controlling feedback. Physics Letters A 170, 421–428.

Ramesh, M., Narayanan, S., 2001. Controlling chaotic motions in a two-dimensional airfoil using time-delayed feedback. Journal of Sound and Vibration 239, 1037–1049.

Rugh, W. J., 1981. Nonlinear Systems Theory, The Volterra–Wiener Approach. The Johns Hopkins University Press.

Scanlan, R.H., Rosenbaum, R., 1951. Introduction to the Study of Aircraft Vibration and Flutter. Macmillan, New York.

Stépán, G., 1989. Retarded Dynamical Systems: Stability and Characteristic Functions, π Pitman Research Notes in Mathematics Series, vol. 210. Longman Scientific and Technical, co-published in the USA with Wiley, New York.

Strganac, T.W., Ko, J., Thompson, D.E., Kurdila, A.J., 2000. Identification and control of limit cycles oscillations in aeroelastic systems. Journal of Guidance, Control, and Dynamics 23, 1127–1133.

Yuan, Y., Yu, P., Librescu, L., Marzocca, P., 2003. Analysis of a 2-D supersonic lifting surface with time delayed feedback control. AIAA Paper 2003-1733, 44th AIAA/ASME/ASCE/ASC Structures, Structural Dynamics, and Materials Conference, April 7–10, 2003, Norfolk, VA, USA.